Electrochimica Acta xxx (2017) 1–8

Contents lists available at ScienceDirect

Electrochimica Acta

journal homepage: www.elsevier.com/locate/electacta

Facilitated proton transfer-electron transfer coupled reactions at thick-film modified electrodes

Franco Martín Zanotto [a, b], Ricardo Ariel Fernández [a, b], Sergio Alberto Dassie [a, b, *]

[a] Departamento de Fisicoquímica, Facultad de Ciencias Químicas, Universidad Nacional de Córdoba, Ciudad Universitaria, X5000HUA, Córdoba, Argentina
[b] Instituto de Investigaciones en Fisicoquímica de Córdoba (INFIQC), CONICET, Ciudad Universitaria, X5000HUA, Córdoba, Argentina

ARTICLE INFO

Article history:
Received 18 September 2017
Received in revised form
26 October 2017
Accepted 16 November 2017
Available online xxx

Keywords:
Facilitated proton transfer
Ion transfer-electron transfer coupled reactions
Thick-film modified electrodes
Protonatable species transfer

ABSTRACT

The theory of cyclic voltammetry of facilitated proton transfer-electron transfer coupled reactions (FPT-ET reactions) in a thick organic film modified electrode is developed. It is shown that the coupling between the facilitated proton transfer-electron transfer processes has a marked effect on the shape of the current-potential profiles. The model allows the analysis of the system in different experimental conditions, such as pH and concentration ratios between the redox probe and the transferring protonated species. This model for proton transfer assisted by different neutral weak bases in a two polarized interfaces system is compared to our previous results for a single polarizable interface. Finally, considerations regarding the application of the thick-film setup are discussed.

1. Introduction

The transfer of protonated species across liquid|liquid interfaces has been studied extensively in recent years, both from the experimental [1–32] and theoretical [11,15,22,23,29,32–36] points of view. In general, these studies have been performed in electrochemical systems with a single polarized interface. However, there are only a few studies related to the transfer of protonated species using an electrochemical setup with two polarized interfaces [37,38]. This is not the case for non-protonatable species. On the one hand, ion transfer in electrochemical experiments with two polarizable liquid|liquid interfaces has been widely studied [39–54]. This electrochemical setup consists of an organic membrane that separates two aqueous solutions. In these interfaces ion transfer-ion transfer coupled reactions take place. On the other hand, three new strategies have been developed involving solid|liquid as well as liquid|liquid interfaces: three-phase electrodes [55–71], thin [30,64,72–84] and thick [85,86] film-modified electrodes. The latter strategies are based on ion transfer-electron transfer coupled reactions using a solid electrode together with two immiscible liquid phases [87–92]. In particular, thick film-modified electrodes are assembled on a conductive substrate fully covered by the thick organic film containing the redox probe, which is immiscible with the aqueous phase. When the redox reaction in the thick film takes place, the electroneutrality of the organic phase is maintained by the injection of cations or anions through the liquid|liquid interface [86]. The thickness of the film allows for the physical separation of the two charge transfer processes, since the diffusion layers do not overlap during the voltammetry experiments. This is achieved performing short experiments with relatively high sweep rates. When one of the injected ions is a proton, one possible mechanism involves the reaction with a weak base, which assists its transfer to the organic phase. This is commonly known as facilitated proton transfer mechanism.

Herein, we present a model of a thick organic film-modified electrode that allows the analysis of facilitated proton transfer-electron transfer coupled reactions (FPT-ET reactions) in different experimental conditions, such as pH and concentration ratios between the redox probe and the transferring protonated species. This model for the proton transfer assisted by different neutral weak bases in a two polarized interfaces system is compared to our previous results calculated for a single polarizable interface [35].

2. Methods

A model considering simultaneous electron transfer at a solid|liquid (S|L) interface and ion transfer at a liquid|liquid (L|L)

* Corresponding author. Departamento de Fisicoquímica, Facultad de Ciencias Químicas, Universidad Nacional de Córdoba, Ciudad Universitaria, X5000HUA, Córdoba, Argentina.
E-mail address: sdassie@fcq.unc.edu.ar (S.A. Dassie).

https://doi.org/10.1016/j.electacta.2017.11.119
0013-4686/

interface and including acid-base equilibria was developed. For simplicity, only single charge processes are taken into consideration. A redox couple is present in the organic phase, initially as an oxidized species (Ox). The acid-base equilibrium of a weak base initially dissolved in the aqueous phase (as the salt HBX) is explicitly incorporated, as well as the explicit HA/A^- buffer. Supporting electrolyte is also explicitly considered in both phases (The organic (OY) and the aqueous (MX)). The possible interfacial equilibria are the following:

$$Ox + e^- \rightleftarrows Red^-$$

$$Cation^+(w) \rightleftarrows Cation^+(o)$$

$$Anion^-(o) \rightleftarrows Anion^-(w)$$

$$B(w) \rightleftarrows B(o)$$

$$HA(w) \rightleftarrows HA(o)$$

where $Cation^+ \equiv M^+; O^+; H^+; HB^+$ and $Anion^- \equiv X^-; Y^-; A^-$ while the homogeneous equilibria are:

$$HB^+(\alpha) \rightleftarrows B(\alpha) + H^+(\alpha)$$

$$HA(\alpha) \rightleftarrows A^-(\alpha) + H^+(\alpha)$$

where α can be the organic or aqueous phase. The following expressions for partition coefficients and acid-base equilibrium constants are incorporated in the model:

$$K_{D,B} = \frac{a_B^O}{a_B^W} \quad (1)$$

$$K_{D,HA} = \frac{a_{HA}^O}{a_{HA}^W} \quad (2)$$

$$K_{a,HB^+}^{\alpha} = \frac{a_B^{\alpha} \cdot a_{H^+}^{\alpha}}{a_{HB^+}^{\alpha}} \quad (3)$$

$$K_{a,HA}^{\alpha} = \frac{a_{A^-}^{\alpha} \cdot a_{H^+}^{\alpha}}{a_{HA}^{\alpha}} \quad (4)$$

In order to deduce the model for facilitated proton transfer-electron transfer coupled reactions, the same set of assumptions as those in a previous paper were made [86]. These correspond to the points (1)–(11) mentioned in Ref. [86]. Assumptions (12) and (13) are included in this work to allow the consideration of acid-base equilibria:

1. The interfaces between the aqueous and the organic phase and between the electrode and organic phase are stationary and planar.
2. Both phases remain quiescent and contain enough inert electrolyte so that mass transport takes place only by diffusion. The potential drop due to solution resistance is neglected, as well as other common electrochemical phenomena such as adsorption and desorption, double layer charge and discharge.
3. The transfer of HO^- ions across the L|L interface is neglected.
4. The partition of the redox species to the aqueous phase, either electrically charged (Red^-) or neutral (Ox), is neglected. Transfer of the other ions and neutral species (B and HA) through the L|L interface is reversible and diffusion controlled, dependent on the Nernst equation or the partition coefficient for the neutral species, respectively.
5. The redox reaction taking place at the electrode surface is reversible and diffusion controlled, dependent on the Nernst equation.
6. The thickness of the organic phase (L) is large enough to avoid overlapping between the diffusion layers of the species generated or consumed on the S|L interface and the L|L interface.
7. Both interfaces present the same surface area, large enough for edge effects to be negligible. Therefore, the semi-infinite linear condition is assumed.
8. Since the electron transfer and ion transfer processes are coupled, the current at both interfaces must be equal.
9. The activity coefficients for all species are assumed to be equal to one.
10. Neither double-layer effects, adsorption, nor ion-pair formation are considered in the model.
11. The applied potential is distributed between the S|L interface and the L|L interface at any time. The potential difference on the former defines the concentration ratio of the redox species and on the latter the ion concentration ratios.
12. pH across the aqueous phase is constant throughout the experiment, depending only on the initial HA/A^- ratio and the aqueous acid dissociation constant of HA.
13. The behaviour of HB^+ as a weak acid can be described using the expression for its acid-base equilibrium constant. All of the acid-base equilibria are fast enough to be considered instantaneous, even when current is flowing.

The S|L interface is defined to be at $x = 0$ and the L|L interface at $x = L$, as shown in Fig. 1. The value of L was set as $12\sqrt{D_{max} t_{max,exp}}$, where D_{max} is the highest of the diffusion coefficients and $t_{max,exp}$ is the maximum duration between all of the simulations, this guarantees that diffusion layers do not overlap. The organic phase contains a redox couple (Ox and Red^-) and both phases can contain all of the remaining species (M^+, X^-, O^+, Y^-, H^+, B, HB^+, HA and A). The protonated weak base and the buffer species are initially dissolved in the aqueous phase as HBX, HA and MA. The organic (OY) and the aqueous (MX) supporting electrolytes are initially dissolved in their respective phases. All of the electrolytes, excepting those involving acid-base equilibria are considered to be completely dissociated. In order to begin the simulations from equilibrium conditions, the distribution potential ($\Delta_o^w \phi_{eq}$) was calculated from the analytical concentrations, the organic phase to aqueous phase volume ratio, $r(= V_o/V_w)$, the acid-base dissociation constants and the standard transfer potential for each ion i ($\Delta_o^w \phi_i^\circ$) by adapting the approach developed in Ref. [93]. All equilibrium concentrations can be calculated from this distribution potential. It is important to note the difference between the analytical concentration of B, c_B^a, which corresponds to the amount of HBX dissolved in the aqueous phase, and the total initial concentration of B, $c_{B,tot}^{init}$, which is a result of the partition and acid-base equilibria of the weak base in the biphasic system, which is highly dependent on the volume ratio [24].

The model's assumptions allow for the simulation of current-potential responses by solving Fick's equations of diffusion for all species in one spatial dimension. Explicit finite difference was used for this work [23,94–96].

The initial potential difference is calculated as the sum of the Galvani potential difference at each interface: $E(0) = \Delta_o^s \phi(0) + [-\Delta_o^w \phi(0)]$ [81,86]. $\Delta_o^s \phi(0)$ is calculated from the initial concentrations of the redox couple Ox and Red^- which are

Please cite this article in press as: F.M. Zanotto, et al., Facilitated proton transfer-electron transfer coupled reactions at thick-film modified electrodes, Electrochimica Acta (2017), https://doi.org/10.1016/j.electacta.2017.11.119

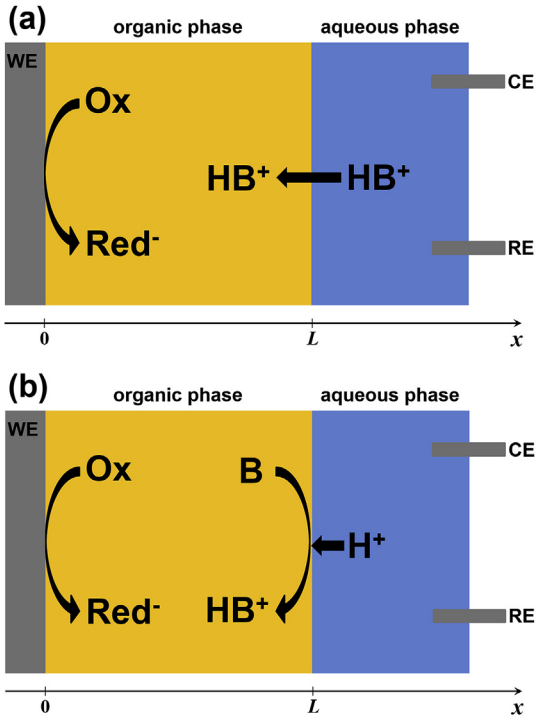

Fig. 1. Schematic representation of the two possible mechanisms involving electron transfer at the S|L interface and ion transfer at the L|L interface. (a) simple transfer mechanism. (b) Facilitated transfer mechanism.

externally fixed, while $\Delta_o^w\phi(0)$ is set equal to the distribution potential at the L|L interface, calculated as described above [86].

The boundary conditions involve the Nernst equation for the coupled processes, i.e. electron transfer and the transfer of ion i:

$$\frac{c_{Ox}(0,t)}{c_{Red^-}(0,t)}\left[\frac{c_i^w(L,t)}{c_i^o(L,t)}\right]^{z_i} = \exp\left\{\frac{F}{RT}\left[E(t) - \Delta_o^s\phi_{Ox}^\circ + \Delta_o^w\phi_i^\circ\right]\right\} \quad (5)$$

where $c_{Ox}(0,t)$ and $c_{Red^-}(0,t)$ are the redox species concentrations at $x = 0$ (S|L interface) at time t, $c_i^w(L,t)$ and $c_i^o(L,t)$ are the concentrations of ion i at $x = L$ (L|L interface) at time t, z_i is the charge of ion i (limited to $+1$ or -1 in this model), $E(t)$ is the externally applied potential, $\Delta_o^s\phi_{Ox}^\circ$ is the standard reduction potential of species Ox and $\Delta_o^w\phi_i^\circ$ is the standard transfer potential of ion i. This condition, together with assumption 11, which can be mathematically expressed as:

$$E(t) = \Delta_o^s\phi(t) + \left[-\Delta_o^w\phi(t)\right] \quad (6)$$

where $\Delta_o^s\phi(t)$ and $\Delta_o^w\phi(t)$ are the Galvani potential differences across the S|L and L|L interfaces at time t, respectively, implies that the electron transfer at the S|L interface satisfies its Nernst equation, as well as each ion at the L|L interface [81,86]. The ratio $\frac{c_{Ox}(x,0)}{c_{Red^-}(x,0)}$ was fixed for all cases as 10^{-6}, since for values lower than 10^{-4}, no significant changes were observed. This allows for the determination of the initial S|L potential difference, and the initial external potential difference, $E(0)$, from Eqs. (5) and (6).

Additional boundary conditions include the flux equality at $x = 0$ for the redox species,

$$D_{Ox}^o\frac{\partial c_{Ox}(0,t)}{\partial x} = -D_{Red^-}^o\frac{\partial c_{Red^-}(0,t)}{\partial x} \quad (7)$$

flux balance at $x = L$ of the weak base species:

$$D_B^o\frac{\partial c_B^o(L,t)}{\partial x} + D_{HB^+}^o\frac{\partial c_{HB^+}^o(L,t)}{\partial x} = D_B^w\frac{\partial c_B^w(L,t)}{\partial x} + D_{HB^+}^w\frac{\partial c_{HB^+}^w(L,t)}{\partial x} \quad (8)$$

and flux equality at $x = L$ for all of the remaining species:

$$D_i^o\frac{\partial c_i^o(L,t)}{\partial x} = D_i^w\frac{\partial c_i^w(L,t)}{\partial x} \quad (9)$$

where i represents each of the ions that are not involved in the acid-base equilibria. Eq. (9) does not apply to species H^+, since its concentration is constant throughout the aqueous phase (assumption (12)).

Assumption (8) requires the current at both interfaces to be equal. This can be expressed mathematically as:

$$D_{H^+}^o\frac{\partial c_{H^+}^o(L,t)}{\partial x} + D_{HB^+}^o\frac{\partial c_{HB^+}^o(L,t)}{\partial x} + \sum_i z_i D_i^o\frac{\partial c_i^o(L,t)}{\partial x} = -D_{Red^-}^o\frac{\partial c_{Red^-}(0,t)}{\partial x} \quad (10)$$

Finally, semi-infinite diffusion conditions imply:

$$c_{Ox}(L,t) = c_{Ox}^{init} \quad (11)$$

$$c_{Red^-}(L,t) = c_{Red^-}^{init} \quad (12)$$

$$c_i^o(0,t) = c_i^o(x,0) \quad (13)$$

$$c_i^w(\infty,t) = c_i^w(x,0) \quad (14)$$

for any species i except Ox and Red^-, where the superindex init denotes initial values for the variable.

A modification of the Powell hybrid method [97–99] was used to solve Eqs. (1)–(14) which describe the boundary conditions for the diffusion differential equations. The time step was chosen in order for the simulation to converge for all tested conditions. The spatial discretization was chosen according to the time step in order for the diffusion equation to be numerically stable ($\Delta x^2/\Delta t D_{max} = 0.45$) [95]. Typical values were $\Delta t = 2\times10^{-4}$s and $\Delta x = 1\times10^{-5}$cm. Results were checked for step size independence. The simulations were carried out in a conventional desktop computer.

In this work, cyclic voltammograms are simulated by applying the following external potential:

$$E(t) = \begin{cases} \Delta_o^s\phi(0) - \Delta_o^w\phi(0) - \nu t & \text{if } t \le \lambda \\ \Delta_o^s\phi(0) - \Delta_o^w\phi(0) + \nu(t-2\lambda) & \text{if } t > \lambda \end{cases} \quad (15)$$

where ν is the potential sweep rate.

In this work, all voltammograms correspond to equal aqueous and organic diffusion coefficients for all species, and the temperature was set to 298.15 K for simplicity.

An analytical expression for the half-wave potential as a function of the most relevant experimental parameters (pH, volume ratio, equilibrium constants, etc) can be derived by adapting the method developed in Refs. [35,36]. This equation will be the subject of a soon to be published article.

3. Results and discussion

The results are presented in four subsections addressing the effect of pH and phase volume ratio on the mid-peak potential

Please cite this article in press as: F.M. Zanotto, et al., Facilitated proton transfer-electron transfer coupled reactions at thick-film modified electrodes, Electrochimica Acta (2017), https://doi.org/10.1016/j.electacta.2017.11.119

(calculated by a simple relation between the peak potentials of the forward and reverse scans: $E_{mid} = \frac{1}{2}(E_{peak}^{forward\ scan} + E_{peak}^{backward\ scan})$) the effect of the initial ratio between concentrations of weak base and redox probe on the facilitated proton transfer-electron transfer coupled reactions, and finally some considerations of the applications of thick-film setup.

3.1. Effect of pH and volume ratio on the mid-peak potential

As it was shown in previous works [85,86] two coupled processes occur in this systems when the working electrode is polarized negatively with respect to the reference electrode. One process occurs only in the organic phase, and involves the reduction of Ox species at S|L interface, resulting in the formation of Red^- species. The other process is necessary in order to maintain electroneutrality in the organic phase, which involves the transfer of ions across the L|L interface. Many of the aspects discussed for non-protonatable ions discussed in these works present the same behaviour as in this model, independently of pH, such as peak-to-peak potential difference and mid-peak potential as a function of initial concentrations, the distribution of applied potential on each interface and successive ion transfer.

For a hydrophobic weak base B, initially dissolved in the aqueous phase, the reduction of Ox species resulting in the formation of Red^- species can be coupled with the simple transfer of the protonated weak base, HB^+, from the aqueous to the organic phase (schematized in Fig. 1(a)). A second possibility involves the reduction of Ox coupled with the mechanism commonly referred to as facilitated proton transfer, which consists in the formation of HB^+ on the organic side of the interface at the expense of weak base B from the organic phase and H^+ from the aqueous phase (schematized in Fig. 1(b)). The former mechanism prevails for low pH values in the aqueous phase, while the latter becomes important at high pH values [24]. It is important to note that, since the aqueous phase is bufferized, the mechanisms proposed are the limiting behaviours of a unique proton transfer reaction. Throughout this work, for simplicity, the pH in the aqueous phase was set by changing the acid dissociation constant of the buffer species, while maintaining their concentrations constant.

The transfer potential for coupled ion transfer-electron transfer processes in general depends on the concentration of both reactants, so as expected, the dependence with the analytical concentration of B, c_B^a , was found to be the same throughout the pH range: E_{mid} is shifted −59 mV for each decade of concentration decrease. This is the same behaviour previously observed for ions that does not present acid-base equilibria in excess with respect to the redox probe [86].

The voltammograms obtained from the simulations show the characteristic peak-to-peak potential difference of around 90 mV described for thick-film modified electrodes [85,86] and liquid membranes [46]. This is independent of which is the prevailing global mechanism of the ion transfer-electron transfer reaction. Fig. 2 shows four exemplary voltammograms for varying pH and typical values of c_B^a and c_{Ox}^{init}, with B in great excess. This figure illustrates the two described mechanisms: for pH = 2.0 and pH = 3.0, E_{mid} remains constant, as expected for the simple transfer mechanism, over which pH has no influence. For pH = 7.0 and pH = 8.0, E_{mid} shifts 59 mV towards negative potentials (i.e., the reduction becomes less spontaneous), this can be expected for a process for which H^+ on the aqueous phase acts as a reactant. This behaviour has been extensively studied with the conventional four electrodes configuration referred hereinafter as ITIES (Interface between Two Immiscible Electrolyte Solutions) [1,3,4,8,13,15,24,28,35,100], and comparing results from both arrangements allows a better understanding of the thick-film system.

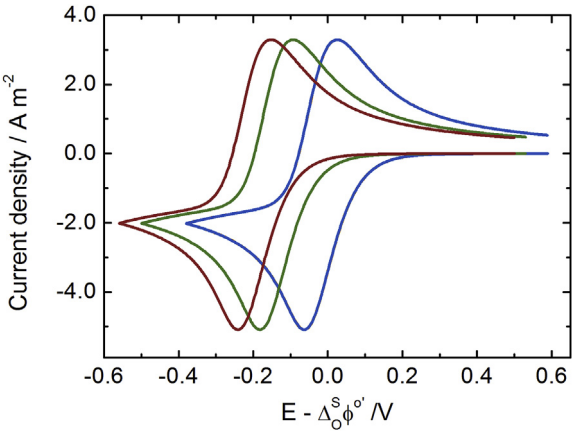

Fig. 2. Voltammograms for the coupled FPT-ET processes at the thick-film electrode corresponding to varying pH values. (———) pH = 2; (———) pH = 3 ; (———) pH = 7 ; (———) pH = 8. Other parameters are as follows: $c_B^a = 0.1M$, $c_{Ox}^{init} = 0.001M$, $pK_{a,HB^+}^W = 7.00$, $K_{D,B} = 100$, $K_{D,HA} = 1 \times 10^{-3}$, $c_{HA,w}^{init} = 0.5M$, $c_{A^-,w}^{init} = 0.5M$, $\Delta_o^w\phi^\circ_{HB^+} = 0.100V$, $\Delta_o^w\phi^\circ_{H^+} = 0.550V$, $\Delta_o^w\phi^\circ_{HO^-} = -0.650V$, $\Delta_o^w\phi^\circ_{A^-} = -0.600V$, $\Delta_o^w\phi^\circ_{M^+} = 0.606V$, $\Delta_o^w\phi^\circ_{X^-} = -0.650V$, $\Delta_o^w\phi^\circ_{O^+} = 0.725V$, $\Delta_o^w\phi^\circ_{Y^-} = -0.699V$, all diffusion coefficients equal to $1 \times 10^{-5}cm^2s^{-1}$.

In order to compare the behaviour of the thick-film experimental setup with the classical ITIES setup, E_{mid} according to the proposed model was plotted as a function of pH in the aqueous phase. This was compared with the half-wave potential according to previous work [35] for the same weak base chemical parameters (K_{a,HB^+}^W, $K_{D,B}$, $\Delta_O^W\phi^{o'}_{HB^+}$, $\Delta_O^W\phi^{o'}_{H^+}$ and equal aqueous and organic diffusion coefficients) at two different volume ratios, (Fig. 3(a)–(c)). For both systems the plots show a few similarities: for low pH values, the transfer potential does not depend on pH, since the simple transfer of HB^+ from the aqueous phase is the predominant process; for higher pH values, a slope with an absolute value of 59 mV is obtained, indicating that the facilitated mechanism is predominant. Since the thick-film setup involves a reduction, the downward trend for its potential represents the same trend in free energy as the ITIES approach. Additionally, it can be observed that E_{mid} does not depend on the volume ratio for the first case (Fig. 3(a)). For thick-film electrodes, the variation of E_{mid} with r is only manifested at high pH values, and is dependent on the concentration ratio between B and Ox. Fig. 3(b) shows that when the weak base is in excess, high values of r yield more negative potentials, while the opposite trend is observed in Fig. 3(c) when the concentration ratio is the opposite of the previous. This behaviour can be readily understood by taking into account two facts: In the first place, when the organic phase volume increases with respect to the aqueous volume at high pH values, the weak base, initially dissolved as HBX in the aqueous phase is diluted in the greater volume of organic phase as neutral specie (B). It is important to note that the initial equilibria, for which a dilution or concentration effect can take place for B, are independent of the experimental setup and the ratio between the analytical concentrations of B and Ox. Secondly, as previously shown [86], when the concentration of the species which is in excess increases, E_{mid} becomes less negative. Thus, in basic solutions, increasing r will decrease the total concentration of weak base, turning E_{mid} more negative when the weak base is in excess and less negative when Ox is in excess.

E_{mid} is not the only important parameter to analyse, since its experimental value can only be obtained if a sufficiently large peak current is detected. This is not always the case for low concentrations of the limiting reactant. Fig. 3(d) shows that for an ITIES system, although E_{mid} is not affected by the volume ratio, the peak current can be very sensitive to it, since it is directly proportional to

Please cite this article in press as: F.M. Zanotto, et al., Facilitated proton transfer-electron transfer coupled reactions at thick-film modified electrodes, Electrochimica Acta (2017), https://doi.org/10.1016/j.electacta.2017.11.119

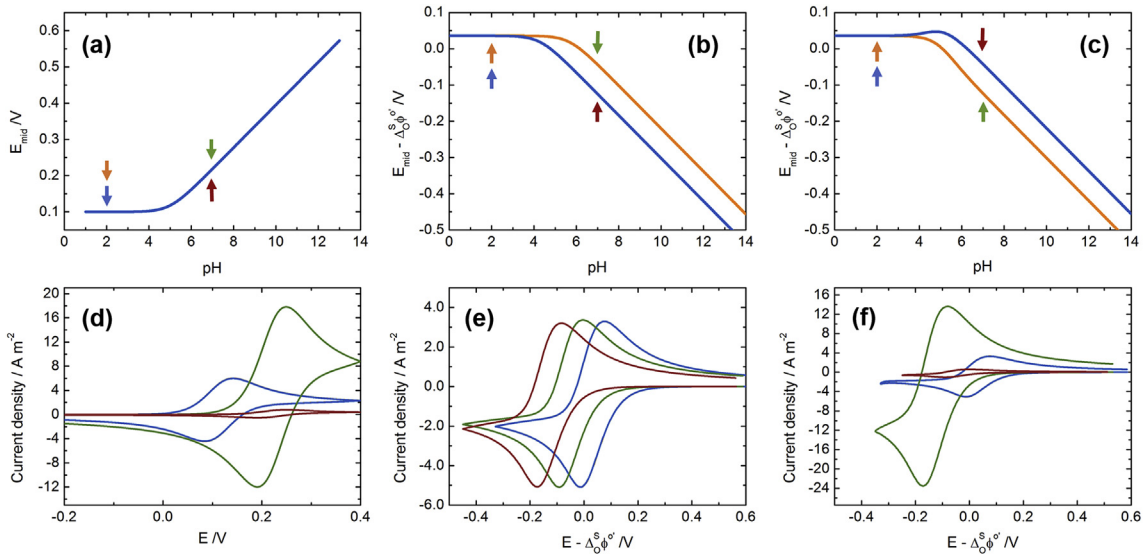

Fig. 3. (a–c) E_{mid} as a function of pH for two different organic to aqueous phase volume ratios. (a) For the ITIES setup according to [35]. $c_B^a = 0.1$ M. (b) For the thick-film setup when the weak base is in excess ($c_B^a = 0.1$ M and $c_{Ox}^{init} = 0.001$ M). (c) For the thick-film setup when the redox probe is in excess ($c_B^a = 0.001$ M and $c_{Ox}^{init} = 0.1$ M). (———) $r = 0.2$; (———) $r = 5.0$. (d–f) Voltammograms corresponding to the highlighted points in the curves above. (———) $r = 0.2$; pH = 2; (———) $r = 5.0$; pH = 2; (———) $r = 0.2$; pH = 7; (———) $r = 5.0$; pH = 7. All other parameters are the same as in Fig. 2. The coloured arrows in (a–c) correspond to the conditions for which the voltammograms in (d–f) were obtained.

the total initial concentration of weak base and this concentration depends on r. Thus, lower current values are observed for voltammograms for which $r > 1$. The dilution or preconcentration effect is not observed for the simple transfer mechanism, since HB^+ remains in the aqueous phase in both cases.

A distinct advantage of the thick-film method is that the peak current depends only on the concentration of the species in defect, so that by maintaining a constant concentration of redox probe, voltammograms at different pH values can be obtained with no change in the peak current, as shown in Fig. 3(e). This allows for the tuning of E_{mid} by using three independent variables: pH, r, and c_{Ox}^{init}, while the peak current only depends on the latter.

In contrast, when Ox is in excess as shown in Fig. 3(f), since the weak base is the limiting reactant, and as its concentration varies, so does the peak current.

3.2. Thick-film setup in excess of weak base

The break-point between the extrapolation of the two linear sections is especially interesting for the estimation of partition coefficients [24]. When $r = 1$, this break-point occurs at the same pH value for the two approaches (ITIES and thick-film). $pH = -\log(K_{a,HB^+}^{W} K_{D,B})$ (for a hydrophobic B). However, this is not the case for different values of r, as shown in Fig. 4 for an excess of weak base. This change arises from the dependence of E_{mid} on the total initial concentration of B. As mentioned before, for low pH values, HB^+ is the predominant species and its concentration throughout the phase does not depend on r, however, for $pH > pK_{a,HB^+}^{W}$ and high $K_{D,B}$ values, the weak base is deprotonated and its initial concentration in the organic phase decreases when r increases. This concentration change produces a potential shift towards the negative side, thus, this break-point moves toward lower pH values. Its value for these conditions emerges as $pH = -\log(rK_{a,HB^+}^{W} K_{D,B})$. This implies that a reliable estimation of $K_{D,B}$ from the break-point requires an accurate determination of r. It is important to note that r does not necessarily correspond to the actual phase volumes present in the electrochemical cell, but to the volumes used in a previous equilibration stage, where both phases are put in contact and stirred in a separate flask. Thus, a wide range of r values can be easily reached [24].

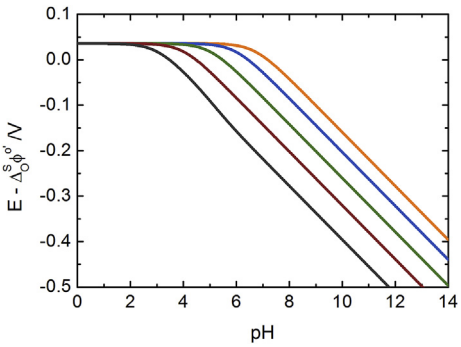

Fig. 4. E_{mid} as a function of pH corresponding to the thick-film setup for different organic to aqueous volume ratios: $r = 0.01$ (———), $r = 0.1$ (———), $r = 1$ (———), $r = 10$ (———) and $r = 100$ (———). In all cases $c_B^a = 0.1$ M and $c_{Ox}^{init} = 0.001$ M. All other parameters are the same as in Fig. 2.

3.3. Thick-film setup in excess of redox probe

Many differences arise with respect to conventional ITIES when the redox species is in excess with respect to B. Fig. 5 shows E_{mid} as a function of pH for the system with a redox species 100 times in excess with respect to the weak base for a greater volume of aqueous (Fig. 5(a)) or organic (Fig. 5(b)) phase.

In both cases the shape of this plot noticeably deviates from the expected for $r = 1$. For the former case, E_{mid} presents a maximum at $pH = -\log(K_{a,HB^+}^{W} K_{D,B})$, which represents a minimum in free energy for the coupled process. This effect emerges due to the dilution of the total initial amount of weak base, which as previously mentioned, shifts the half-wave potential towards more positive values. The trend is cancelled off by the downwards slope as pH increases, thus produce a maximum in the curve. Its position corresponds to an initial condition for which the initial concentrations of B in the organic phase and HB^+ in the aqueous phase are equal. This results in both mechanisms taking place at the same rate, since all diffusion coefficients are equal.

An opposing behaviour is encountered for low r values, that is, with a greater volume of aqueous phase (Fig. 5(b)). While the

Please cite this article in press as: F.M. Zanotto, et al., Facilitated proton transfer-electron transfer coupled reactions at thick-film modified electrodes, Electrochimica Acta (2017), https://doi.org/10.1016/j.electacta.2017.11.119

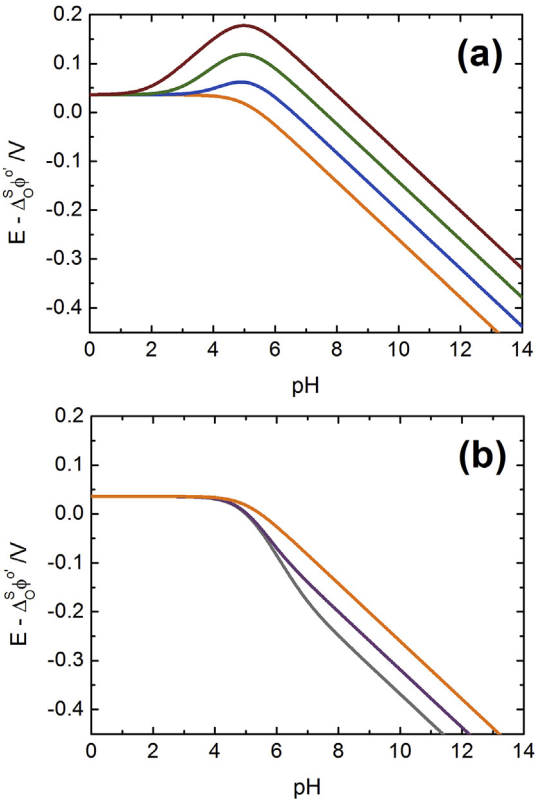

Fig. 5. E_{mid} as a function of pH corresponding to the thick-film setup. (a) With a greater organic phase volume: $r = 1$ (——), $r = 10$ (——), $r = 100$ (——), $r = 1000$ (——). (b) With a greater aqueous phase volume: $r = 0.01$ (——), $r = 0.1$ (——), $r = 1$ (——). In all cases $c_B^a = 0.1$ M and $c_{Ox}^{init} = 0.001$ M. All other parameters are the same as in Fig. 2.

break-point between the extrapolated linear plots remains at $pH = -\log(K^W_{a,HB^+} K_{D,B})$, for basic solutions two distinct slopes are clearly discerned, divided by an additional break-point that can be as high as $pH = -\log(K^W_{a,HB^+})$, depending on the value of r. While the second linear section remains with a slope of −59 mV, the first one reaches a value of around −118 mV.

3.4. Applications

A good understanding of this system through the analysis of the model can be exploited in order to determine thermodynamic parameters. The case involving the determination of $K_{D,B}$ will be developed as an example. A very direct approach that can be used in the ITIES system is the construction of the E_{mid} vs. pH curve, from which the break-point between the two linear regions can be extracted, for which $pH = -\log(K_{D,B}K^W_{a,HB^+})$. The value of K^W_{a,HB^+} can be easily determined from aqueous acid-base titration, and thus, the value of $K_{D,B}$ is calculated. However, it is not always possible to find this break-point, since it might be too low or too high for two linear slopes to be reliably fitted, or the supporting electrolyte might become a significant interferent. The thick-film setup can be used to overcome both of these limitations. Our analysis will be centred on conditions for which the weak base is in excess with respect to the redox probe, since this has been more widely explored in experiments [77,79,85].

An example of the first case is the transfer of anhydrotetracycline (AHTC) across the water|1,2-dichloroethane, for which $pK^W_{a,HAHTC^+} = 3.23 \pm 0.08$ [101] and $\log(K_{D,AHTC}) = 2.4 \pm 0.1$ [26]. Several ITIES experiments would have to be carried out for a pH range below the resulting break-point of 0.8 in order to accurately determine $K_{D,AHTC}$, which is not feasible (Fig. 6(a)). The thick-film methodology however, allows for the controlled shift of this value towards a pH as high as 2.3, when the volume ratio equals 30 as seen in Fig. 6(b). As long as the phase volumes used in the equilibration stage are accurately measured, this strategy can be employed to find more convenient experimental conditions, and thus, more accurate values for $K_{D,B}$. Another similar example of pharmaceutical interest is O-methyl piroxicam, with $pK^W_{a,HB^+} = 2.72$ and $\log(K_{D,B}) = 2.07$ [10] for which a similar approach can be employed (details are presented in the Supplementary Material).

The second case is exemplified by the transfer of the weak base tylosin B across the same water|1,2-dichloroethane interface, ($pK^W_{a,HTyl^+} = 8.36$ [102] and $\log\left(K_{D,Tyl}\right) = 2.1 \pm 0.1$ [28]) for which the slope of 59 mV cannot be observed when using tetrapentylammonium dicarbollylcobaltate as supporting electrolyte in the organic phase, since the mid-peak potential shifts outside the polarizable potential window as pH increases. Fig. 7(a) shows the corresponding E_{mid} vs. pH plot according to the model for ITIES systems [35], with parameters corresponding to tylosin B. The dashed line indicates an estimate for the maximum observable value of E_{mid}. According to this plot, a very narrow range involving a facilitated ion transfer can be studied using the ITIES cell (of around one pH unit). This range can be extended in the thick-film approach by tuning only the species concentration ratio, as shown in Fig. 7(b). In this figure, the dotted line represents again values attainable by the use of the same supporting electrolyte in the same concentration. A shift of E_{mid} of around 90 mV can be achieved by changing c_B^a or c_{Ox}^{init} by a factor of 30, which is enough to obtain a pH range of around 2.5 units for which the facilitated mechanism can be

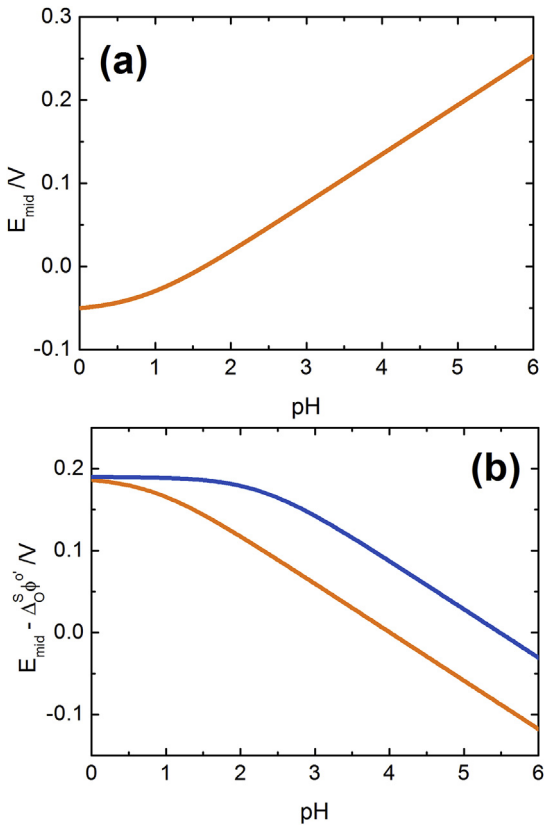

Fig. 6. Expected mid-peak potential vs. pH response for AHTC in a water|1,2-dichloroethane interface for (a) the ITIES setup and (b) for the thick-film setup: $r = 1$ (——), $r = 0.03$ (——).

Please cite this article in press as: F.M. Zanotto, et al., Facilitated proton transfer-electron transfer coupled reactions at thick-film modified electrodes, Electrochimica Acta (2017), https://doi.org/10.1016/j.electacta.2017.11.119

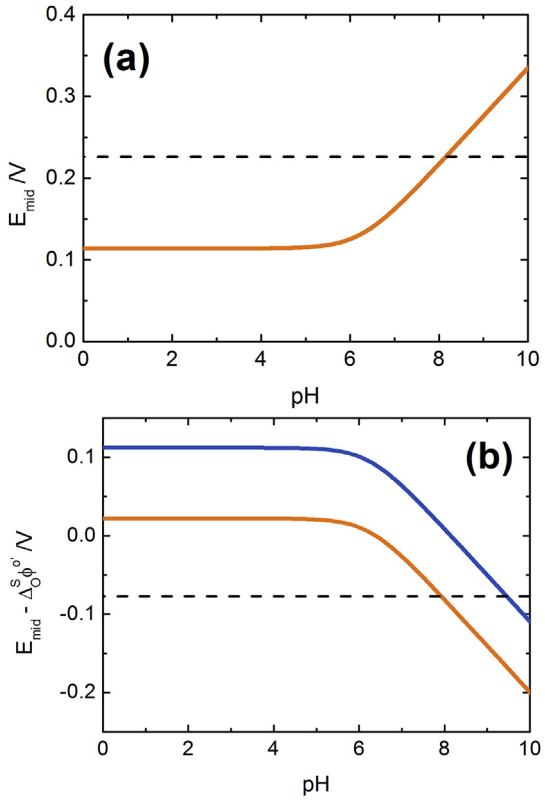

Fig. 7. Expected mid-peak potential vs. pH response for tylosin B in a water|1,2-dichloroethane interface for (a) the ITIES setup and (b) for the thick-film setup: $c_B^a/c_{Ox}^{init} = 100$ (———), $c_B^a/c_{Ox}^{init} = 3000$ (———) The dashed line represents an estimation of the (a) maximum (b) minimum potential observable when a typical concentration of tetrapentylammonium dicarbollylcobaltate is used as a supporting electrolyte.

observed. In this way, a linear slope can be adjusted and a reliable value for $K_{D,B}$ easily determined. It is worth noting that this range could be extended even further by diminishing the supporting electrolyte concentration, according to the guidelines provided in a previous report [86].

4. Conclusion

A theoretical model of thick-film modified electrodes taking into account the acid base equilibria of a hydrophobic weak base initially dissolved in the aqueous phase and a redox couple present in the organic phase is presented.

The external applied potential difference is distributed between the solid|liquid and the liquid|liquid interfaces. Thus, the obtained current-potential profiles are as expected for two polarizable interfaces, and depend on the initial concentration ratio between the redox probe and the total initial concentration of the weak base.

The main difference between using a protonatable weak base as transferring species instead of a permanent ion in a thick-film modified electrode, are the possibility of pre-concentrate (or dilute) the base, and also adjust the relative amounts of charged and neutral species, by handling the pH and the volume ratio. The relationship of facilitated proton transfer-electron transfer coupled reactions in this set up with these external variables was described. Hence, as an application with experimental interest, the possibility of tuning mid-peak potential with the volume ratio offered a practical strategy to shift the mid-peak potential vs pH profile, and estimate partition coefficients of drugs which would not be accessible with the conventional ITIES setup.

Additionally, the present model can be extended by including kinetic parameters for the degradation of weak bases, and could be used as a simple method to study drug stability in solution, i.e. accelerated acid hydrolysis, under different experimental conditions.

Acknowledgements

R.A.F. and S.A.D. are Researchers from Consejo Nacional de Investigaciones Científicas y Tecnológicas (CONICET). F.M.Z. thanks CONICET for the fellowship granted. Financial support from CONICET (PIP 00174), Secretaria de Ciencia y Tecnología de la Universidad Nacional de Córdoba (SECyT-UNC) and Fondo para la Investigación Científica y Tecnológica PICT-2012-1820 are gratefully acknowledged.

Appendix A. Supplementary data

Supplementary data related to this article can be found at https://doi.org/10.1016/j.electacta.2017.11.119.

References

[1] E. Makrlik, W. Ruth, P. Vanýsek, Electrochim. Acta 28 (1983) 575–577.
[2] Z. Yoshida, H. Freiser, J. Electroanal. Chem. 162 (1984) 307–319.
[3] D. Homolka, V. Mareček, Z.Z. Samec, K. Baše, H.H. Wendt, J. Electroanal. Chem. 163 (1984) 159–170.
[4] Y. Liu, E. Wang, J. Chem. Soc. Faraday Trans. I 83 (1987) 2993–2999.
[5] E. Makrlík, J. Colloid Interface Sci. 137 (1990) 30–35.
[6] H. Doe, K. Yoshioka, T. Kitagawa, J. Electroanal. Chem. 324 (1992) 69–78.
[7] L.M. Yudi, A.M. Baruzzi, J. Electroanal. Chem. 328 (1992) 153–164.
[8] K. Kontturi, L. Murtomäki, J. Pharm. Sci. 81 (1992) 970–975.
[9] L.M. Yudi, A.M. Baruzzi, V.M. Solis, J. Electroanal. Chem. 360 (1993) 211–219.
[10] F. Reymond, G. Steyaert, A. Pagliara, P. Carrupt, B. Testa, H.H. Girault, Helv. Chim. Acta 79 (1996) 1651–1669.
[11] F. Reymond, P.-F. Brevet, P.-A. Carrupt, H.H. Girault, J. Electroanal. Chem. 424 (1997) 121–139.
[12] Z. Ding, F. Reymond, P. Baumgartner, D.J. Fermín, P.-F. Brevet, P. Carrupt, H.H. Girault, Electrochim. Acta 44 (1998) 3–13.
[13] Y. Kubota, H. Katano, K. Maeda, M. Senda, Electrochim. Acta 44 (1998) 109–116.
[14] Z. Samec, J. Langmaier, A. Trojánek, E. Samcová, J. Málek, Anal. Sci. 14 (1998) 35–41.
[15] S. Sawada, T. Osakai, Phys. Chem. Chem. Phys. 1 (1999) 4819–4825.
[16] F. Reymond, P.-A. Carrupt, B. Testa, H.H. Girault, Chem. Eur. J. 5 (1999) 39–47.
[17] A.I. Azcurra, L.M. Yudi, A.M. Baruzzi, J. Electroanal. Chem. 461 (1999) 194–200.
[18] W. Wickler, A. Mönner, E. Uhlemann, S. Wilke, H. Müller, J. Electroanal. Chem. 469 (1999) 91–96.
[19] M. Senda, Y. Kubota, H. Katano, in: Liq. Interfaces Chem. Biol. Pharm. Appl, 2001, pp. 683–698.
[20] Y. Kubota, H. Katano, M. Senda, Anal. Sci. 17 (2001) 65–70.
[21] R.A. Fernández, S.A. Dassie, J. Electroanal. Chem. 585 (2005) 240–249.
[22] T. Osakai, T. Hirai, T. Wakamiya, S. Sawada, Phys. Chem. Chem. Phys. 8 (2006) 985–993.
[23] J.I. Garcia, R.A. Iglesias, S.A. Dassie, J. Electroanal. Chem. 586 (2006) 225–236.
[24] J.I. Garcia, R.A. Fernández, A.J. Ruggeri, S.A. Dassie, J. Electroanal. Chem. 594 (2006) 80–88.
[25] M. Rimboud, C. Elleouet, F. Quentel, J.-M. Kerbaol, M. L'Her, J. Electroanal. Chem. 622 (2008) 233–237.
[26] R.A. Fernández, S.A. Dassie, J. Electroanal. Chem. 624 (2008) 121–128.
[27] B. Su, F. Li, R. Partovi-Nia, C. Gros, J.-M. Barbe, Z. Samec, H.H. Girault, Chem. Commun. (2008) 5037–5038.
[28] R.A. Fernández, M.I. Velasco, L.I. Rossi, S.A. Dassie, J. Electroanal. Chem. 650 (2010) 47–54.
[29] J.I. Garcia, M.B. Oviedo, S.A. Dassie, J. Electroanal. Chem. 645 (2010) 1–9.
[30] J. Gu, W. Zhao, Y. Chen, X. Zhang, X. Xie, S. Liu, X. Wu, Z. Zhu, M. Li, Y. Shao, Anal. Chem. 87 (2015) 11819–11825.
[31] F. Vega Mercado, J.M. Ovejero, R.A. Fernández, S.A. Dassie, J. Electroanal. Chem. 765 (2016) 100–104.
[32] F. Vega Mercado, J.M. Ovejero, F.M. Zanotto, M.R. Serial, M.I. Velasco, R.A. Fernández, R.H. Acosta, S.A. Dassie, J. Electroanal. Chem. 791 (2017) 64–74.
[33] S.A. Dassie, J. Electroanal. Chem. 578 (2005) 159–170.
[34] S.A. Dassie, J. Electroanal. Chem. 585 (2005) 256–268.
[35] S.A. Dassie, J. Electroanal. Chem. 728 (2014) 51–59.
[36] F. Vega Mercado, F.M. Zanotto, R.A. Fernández, S.A. Dassie, J. Electroanal.

Chem. 774 (2016) 111–121.
[37] T.D. Chung, F.C. Anson, Anal. Chem. 73 (2001) 337–342.
[38] A.M. Collins, X. Zhang, J.J. Scragg, G.J. Blanchard, F. Marken, ChemPhysChem 11 (2010) 2862–2870.
[39] O. Shirai, S. Kihara, M. Suzuki, K. Ogura, M. Matsui, Anal. Sci. 7 (Suppl.) (1991) 607–610.
[40] V. Horváth, G. Horvai, Anal. Chim. Acta 273 (1993) 145–152.
[41] O. Shirai, S. Kihara, Y. Yoshida, M. Matsui, J. Electroanal. Chem. 389 (1995) 61–70.
[42] O. Shirai, Y. Yoshida, M. Matsui, K. Maeda, S. Kihara, Bull. Chem. Soc. Jpn. 69 (1996) 3151–3162.
[43] T. Kakiuchi, Electrochim. Acta 44 (1998) 171–179.
[44] C. Beriet, H.H. Girault, J. Electroanal. Chem. 444 (1998) 219–229.
[45] S. Amemiya, Z. Ding, J. Zhou, A.J. Bard, J. Electroanal. Chem. 483 (2000) 7–17.
[46] Z. Samec, A. Trojánek, J. Langmaier, E. Samcová, J. Electroanal. Chem. 481 (2000) 1–6.
[47] M.H. Barker, L. Murtomäki, K. Kontturi, J. Electroanal. Chem. 497 (2001) 61–68.
[48] S.M. Ulmeanu, H. Jensen, Z. Samec, G. Bouchard, P.-A. Carrupt, H.H. Girault, J. Electroanal. Chem. 530 (2002) 10–15.
[49] N. Ichieda, O. Shirai, M. Kasuno, K. Banu, A. Uehara, Y. Yoshida, S. Kihara, J. Electroanal. Chem. 542 (2003) 97–107.
[50] N. Ichieda, O. Shirai, Y. Yoshida, K. Maeda, M. Torimura, S. Kihara, Electroanalysis 16 (2004) 779–782.
[51] A. Molina, J.A. Ortuño, C. Serna, E. Torralba, J. Gonzalez, Electroanalysis 22 (2010) 1634–1642.
[52] A. Molina, J.A. Ortuño, C. Serna, E. Torralba, Phys. Chem. Chem. Phys. 12 (2010) 13296–13303.
[53] E. Torralba, J.A. Ortuño, C. Serna, J. González, A. Molina, Electroanalysis 23 (2011) 2188–2196.
[54] A. Molina, C. Serna, J.A. Ortuno, E. Torralba, Annu. Rep. Sect. C Phys. Chem. 108 (2012) 126–176.
[55] F. Marken, R.D. Webster, S.D. Bull, S.G. Davies, J. Electroanal. Chem. 437 (1997) 209–218.
[56] F. Scholz, Š. Komorsky-Lovrić, M. Lovrić, Electrochem. Commun. 2 (2000) 112–118.
[57] V. Mirčeski, R. Gulaboski, F. Scholz, Electrochem. Commun. 4 (2002) 814–819.
[58] M. Donten, Z. Stojek, F. Scholz, Electrochem. Commun. 4 (2002) 324–329.
[59] G. Bouchard, A. Galland, P.-A. Carrupt, R. Gulaboski, V. Mirčeski, F. Scholz, H.H. Girault, Phys. Chem. Chem. Phys. 5 (2003) 3748–3751.
[60] R. Gulaboski, A. Galland, K. Caban, A. Kretschmer, P.-A. Carrupt, Z. Stojek, H.H. Girault, F. Scholz, J. Phys. Chem. B 108 (2004) 4565–4572.
[61] Š. Komorsky-Lovrić, V. Mirčeski, C. Kabbe, F. Scholz, J. Electroanal. Chem. 566 (2004) 371–377.
[62] F. Quentel, V. Mirčeski, C. Elleouet, M. L'Her, J. Phys. Chem. C 112 (2008) 15553–15561.
[63] H. Deng, X. Huang, L. Wang, Langmuir 26 (2010) 19209–19216.
[64] F. Quentel, V. Mirčeski, M. L'Her, K. Stankoska, J. Phys. Chem. C 116 (2012) 22885–22892.
[65] K. Hu, B. Xu, H. Shao, Electrochem. Commun. 50 (2015) 36–38.
[66] Q. Fulian, J.C. Ball, F. Marken, R.G. Compton, A.C. Fisher, Electroanalysis 12 (2000) 1012–1016.
[67] Š. Komorsky-Lovrić, M. Lovrić, F. Scholz, Collect. Czechoslov. Chem. Commun. 66 (2001) 434–444.
[68] Š. Komorsky-Lovrić, M. Lovrić, F. Scholz, J. Electroanal. Chem. 508 (2001) 129–137.
[69] J.C. Myland, K.B. Oldham, J. Electroanal. Chem. 530 (2002) 1–9.
[70] M. Lovrić, F. Scholz, J. Electroanal. Chem. 540 (2003) 89–96.
[71] V. Mirčeski, R. Gulaboski, F. Scholz, J. Electroanal. Chem. 566 (2004) 351–360.
[72] C. Shi, F.C. Anson, Anal. Chem. 70 (1998) 3114–3118.
[73] C. Shi, F.C. Anson, J. Phys. Chem. B 102 (1998) 9850–9854.
[74] H.O. Shafer, T.L. Derback, C. a. Koval, J. Phys. Chem. B 104 (2000) 1025–1032.
[75] F. Quentel, V. Mirčeski, M. L'Her, Anal. Chem. 77 (2005) 1940–1949.
[76] R. Gulaboski, V. Mirčeski, C.M. Pereira, M.N.D.S. Cordeiro, A.F. Silva, F. Quentel, M. L'Her, M. Lovrić, Langmuir 22 (2006) 3404–3412.
[77] M. Zhou, S. Gan, L. Zhong, B. Su, L. Niu, Anal. Chem. 82 (2010) 7857–7860.
[78] L. Zhong, M. Zhou, S. Gan, Y. Bao, X. Dong, L. Niu, L. Guo, Electrochem. Commun. 13 (2011) 221–224.
[79] S. Gan, M. Zhou, J. Zhang, L. Zhong, J. Ulstrup, L. Niu, Electroanalysis 25 (2013) 857–866.
[80] V. Mirceski, B. Mitrova, V. Ivanovski, N. Mitreska, A. Aleksovska, R. Gulaboski, J. Solid State Electrochem 19 (2015) 2331–2342.
[81] V. Mirčeski, F. Quentel, M. L'Her, A. Pondaven, Electrochem. Commun. 7 (2005) 1122–1128.
[82] Š. Komorsky-lovrić, M. Lovrić, Cent. Eur. J. Chem. 3 (2005) 216–229.
[83] M. Lovrić, Š. Komorsky-Lovrić, J. Solid State Electrochem. 10 (2006) 852–856.
[84] Š. Komorsky-Lovrić, M. Lovrić, ChemElectroChem 1 (2014) 436–440.
[85] M. Zhou, S. Gan, L. Zhong, X. Dong, J. Ulstrup, D. Han, L. Niu, Phys. Chem. Chem. Phys. 14 (2012) 3659.
[86] F.M. Zanotto, R.A. Fernández, S.A. Dassie, J. Electroanal. Chem. 784 (2017) 25–32.
[87] C.E. Banks, T.J. Davies, R.G. Evans, G. Hignett, A.J. Wain, N.S. Lawrence, J.D. Wadhawan, F. Marken, R.G. Compton, Phys. Chem. Chem. Phys. 5 (2003) 4053–4069.
[88] M. Opallo, A. Lesniewski, J. Niedziolka, E. Rozniecka, G. Shul, Rev. Polarogr. 54 (2008) 21–30.
[89] F. Scholz, Annu. Rep. Prog. Chem. Sect. C 102 (2006) 43–70.
[90] D. Kaluza, W. Adamiak, M. Opallo, M. Jonsson-Niedziolka, Electrochim. Acta 132 (2014) 158–164.
[91] F. Scholz, U. Schröder, R. Gulaboski, A. Doménech-Carbó, Electrochemistry of Immobilized Particles and Droplets, second ed., Springer, New York, 2015.
[92] H. Tian, Y. Li, H. Shao, H.Z. Yu, Anal. Chim. Acta 855 (2015) 1–12.
[93] J.I. Garcia, R.A. Fernández, S.A. Dassie, T. Kakiuchi, J. Electroanal. Chem. 640 (2010).
[94] D.K. Gosser, Cyclic Voltammetry: Simulation and Analysis of Reaction Mechanisms, VCH publishers, New York, 1993.
[95] D. Britz, Digital Simulation in Electrochemistry, third ed., Springer, Berlin Heidelberg, 2005.
[96] A.J. Bard, C.R. Faulkner, Electrochemical Methods, Fundamentals and Applications, second ed., John Wiley & Sons, New York, 2001.
[97] A.M. Ostrowski, Solution of Equations and System of Equations, 2sd Ed, Academic Press Inc, 1966.
[98] W.H. Press, S.A. Teukolsky, I.T. Vetterling, B.P. Flannery, Numerical Recipes in Fortran 77 the Art of Scientific Computing, second ed., Cambridge University Press, 1992.
[99] Subroutines Fortran Are Free Available, 2017. http://www.netlib.org.
[100] F. Reymond, G. Steyaert, P.-A. Carrupt, B. Testa, H.H. Girault, J. Am. Chem. Soc. 118 (1996) 11951–11957.
[101] J.M. Siqueira, S. Carvalho, E.B. Paniago, L. Tosi, H. Beraldo, J. Pharm. Sci. 83 (2008) 291–295.
[102] J.W. McFarland, C.M. Berger, S.A. Froshauer, S.F. Hayashi, S.J. Hecker, B.H. Jaynes, M.R. Jefson, B.J. Kamicker, C.A. Lipinski, K.M. Lundy, C.P. Reese, C.B. Vu, J. Med. Chem. 40 (1997) 1340–1346.

Please cite this article in press as: F.M. Zanotto, et al., Facilitated proton transfer-electron transfer coupled reactions at thick-film modified electrodes, Electrochimica Acta (2017), https://doi.org/10.1016/j.electacta.2017.11.119